Aromatic Polymers Obtained by Precipitation Polycondensation. 3. Thermal Behavior and Microstructure of PEKEKK Particles

D. R. Rueda, M. G. Zolotukhin, M. E. Cagiao, and F. J. Balta Calleja*

Instituto de Estructura de la Materia, C.S.I.C., Serrano 119, Madrid 28006, Spain

D. Villers and M. Dosière

Université de Mons−Hainaut, Phys.-Chem. des Polymeres, Place du Parc 20, B-3000 Mons, Belgium

Received March 29, 1996; Revised Manuscript Received July 30, 1996[⊗]

ABSTRACT: In the second part of this series the influence of monomer concentration on the chemical structure and the shape and size of poly(aryl ether ketone ether ketone ketone) (PEKEKK) particles was reported. The present study of the thermal behavior and microstructure of aromatic polyketone samples in the form of particles has been carried out by means of differential scanning calorimetry (DSC) and wide angle X-ray diffraction (WAXD). Samples before and after reprecipitation and annealing were investigated. Similar to other polyketones, PEKEKK shows two polymorphic forms: form II, less stable, is currently observed in the samples, while the reprecipitated polymer preferentially shows form I. Form II is partially converted into form I upon short annealing treatment of the material. The semicrystalline materials show melting points and glass transition temperatures which are higher for the samples with higher molecular weight and more regular chain structure. A comparison of thermal properties of "as obtained" and "reprecipitated" samples reveals the influence of the particle architecture on the chain mobility. The latter determines the ability of polyketone chains to crystallize. Infrared dichroism was also used to characterize the arrangement of polymer chains inside the polyketone particles showing crystal habits.

Introduction

Aromatic poly(ether ketone)s as high-performance thermoplastic materials have received special attention in the last decade.[1−3] These polymers show high thermostability and resistance to chemical agents[2,3] and are usually semicrystalline. A basic interest for polyketones was also prompted by the fact that polyketones show a double melting behavior[4−6] when crystallized at temperatures above the glass transition temperature. The origin of this phenomenon is still open to discussion.

With reference to the structure physical properties correlation it is known that the thermal properties (melting and glass transition temperatures) of para-linked aromatic polyketones are very dependent on the ether/ketone ratio which influences the lattice parameters of the orthorhombic unit cell. The chain packing is similar to that found for poly(phenylene oxide)[7] and for PEEK.[8−10] For other aromatic polyketones the *b* and *c* lattice parameters increase linearly with the carbonyl content while the *a* parameter decreases. For polyketones with a carbonyl content larger than 50% (PEKEKK and PEKK) Blundell and Newton[11] observed additional reflections in the X-ray pattern of oriented samples which were indexed in terms of a new orthorhombic crystallographic form with the *a* and *b* axes exchanged with each other.

Gardner et al. reported new results on the polymorphism of aromatic polyketones with different ether/ketone ratios[12,13] crystallized under different conditions, and more recently for polyketones containing isophthalic units.[14] In the case of polyketones crystallized from the melt the first orthorhombic packing (PEEK-type) is always observed for all polyketones independently of their carbonyl content. On the other hand, samples prepared by cold crystallization (from amorphous material upon thermal treatement) and solvent crystallization, with a carbonyl content larger than 50% (PEKEKK, PEKK), showed exclusively the second crystallographic form. For the polyketone PEK the first crystallographic form is still predominant in relation to the second one. In this paper we will refer to these polymorphic forms as form I and form II following Gardner's notation.

It is assumed that aromatic polyketones are linear, with para substitution in arylene rings of the main chain. Nevertheless, regardless of the preparation method (nucleophilic or electrophilic routes) defect isomeric structures can be present along the linear polyketone chains. The presence of these defect structures, even in small relative amounts can obviously affect the chain packing and relative motion of chains and, consequently, the microstructure and thermal behavior of the material. In the second paper of this series[15] the preparation and NMR characterization of the aromatic polyketones investigated here were reported. Such a detailed chemical characterization confirmed a good quality and homogeneity of the materials, and it encouraged us to investigate the variation of the thermal properties and the microstructure as a function of (a) the molecular weight and chain regularity and (b) the architecture of the particles obtained. Thus, a characterization of the polyketone samples by means of X-ray diffraction and differential scanning calorimetry is presented. Infrared dichroism was also used for a better characterization of the building up of polyketone particles which showed a needlelike crystal habit.

* To whom correspondence is addressed.

† Part 2: M. G. Zolotukhin et al. (submitted for publication to Macromol. Chem., Phys.).

⊗ Abstract published in *Advance ACS Abstracts,* September 15, 1996.

S0024-9297(96)00482-2 CCC: $12.00

Table 1

sample	viscosity η_{inh} (dL/g)	defect isomer molar content (%)
P1	1.46	6.7
P2	1.85	5.0
P3	2.42	2.4

Experimental Part

Materials. The chemical repeat unit of poly(aryl ether ketone ether ketone ketone) is

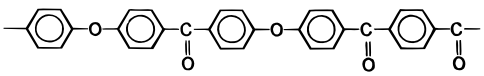

PEKEKK

Three PEKEKK samples prepared by the precipitation polycondensation method were investigated. The samples obtained in particle form show different molecular weights (viscosity) and different isomer unit contents (Table 1). The isomer unit content refers to the relative total amount of 1,2 and 1,3 substituted phenylene rings. A description of the preparation and characterization of samples is given elsewhere.[15]

Let us remember here that both the shape and the size of the particles were found to be governed by reaction conditions. The P1 sample consists of smooth, elongated particles (0.4−0.7 mm). The P2 sample consists of spherical particles of about 0.1 mm diameter in the form of elongated aggregates (<1 mm long). The P3 sample in addition to the aggregates of spherical particles shows very thin needlelike crystals.

Methods. For the thermal study a differential scanning calorimeter Perkin-Elmer DSC-4 was employed. A heating rate of 20 K/min was used. After the first DSC run the sample was rapidly cooled to 90 °C and then a second DSC run was made at the same heating rate. DSC pans, carefully filled with polymer particles, contained about 5−8 mg of material.

To examine the role of the architecture of the particles themselves on the properties, the materials were dissolved in a $CF_3COOH-CDCl_3$ mixture and reprecipitated using methanol.

A vertical powder diffractometer (Rigaku) was used to obtain wide angle X-ray diffractograms (WAXD) using a Cu Kα, Ni-filtered radiation source from a rotating anode working at 8 kW. A scanning speed of 1° (2θ) per min was used. To overcome the difficulties in filling the sample holder with the same amount of the particle sample, we have prepared sintered disks (ϕ = 13 mm) using 100 mg of material. For sintering, the samples were evacuated for 5 min followed by application of a pressure of 0.75 MPa under vacuum for another 5 min. Thus, X-ray diffratograms from sintered samples are more comparable and reliable than those directely obtained from particle samples. The crystallinity of the samples was calculated as the ratio of the crystalline area to the total diffracted area after subtraction of a linear background within the angular region between 5 and 36° (2θ). To separate both the crystalline and amorphous contribution from the experimental scattering pattern, we have considered an amorphous halo centered at 20° (2θ) which tangentially approaches the experimental curve at 2θ values of 14, 26, and 35°.

In order to promote crystallinity, all the sintered samples and the reprecipitated material were annealed at 230 °C for 15 min. Particularly, sample P3 was thermally treated up to temperatures closer to the melting point to study the polymorphism.

A flat camera was also used to obtain X-ray patterns of the particle samples, which were inserted in a glass capillary (2 and 0.7 mm diameter). A distance from the sample to X-ray film of 40 mm was used.

Polarized infrared spectra of P3 needlelike particles were obtained on a Bruker IFS 113V FTIR spectrometer using an aluminum wire grid polarizer. The spectra were obtained after 32 accumulated scans with a resolution of 2 cm^{-1}. The longest particle size was taken as the reference axis when irradiated with polarized light.

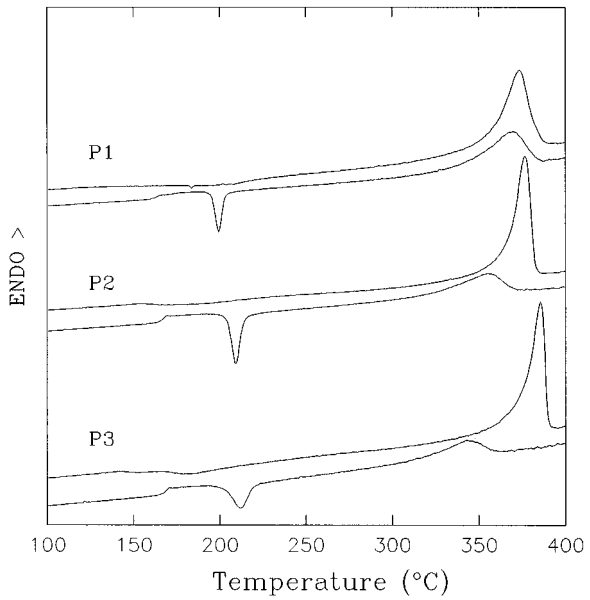

Figure 1. First (top) and second (bottom) DSC heating scans for the three different aromatic polyketones.

Table 2. Thermal Properties from the First and Second DSC Runs of Polyketones "As Obtained": Melting, T_m, Glass Transition, T_g, and Crystallization Peak, T_c, Temperatures; Heat of Fusion, ΔH, and Heat of Crystallization, ΔH_c

	first DSC scan		second DSC scan				
sample	T_m (°C)	ΔH (J/g)	T_g (°C)	T_c (°C)	ΔH_c (J/g)	T_m (°C)	ΔH (J/g)
P1	373.5	59.1	162.5	199.4	−9.7	369.9	31.7
P2	376.6	60.3	166.5	209.2	−16.8	353.3	23.4
P3	385.6	61.5	168.0	212.1	−15.4	342.5	15.8

Results

Thermal Behavior. Figure 1 shows the first DSC traces from polymers and the consecutive second scans after a rapid cooling (320 K/min) of the sample to 90 °C. The glass transition and melting temperatures and the enthalpies of fusion are shown in Table 2. For these three polymers the first DSC runs show a small, very broad exotherm (150−180 °C) and melting points at 374, 377, and 386 °C, respectively. The small broad exotherms are associated with some reorganization processes upon heating the material. The melting point and the heat of fusion of the polyketones increase with increasing molecular weight. The second DSC scans show a well-defined glass transition followed by a rather sharp cold crystallization peak and finally by a broad melting peak. The glass transition, T_g, and the crystallization peak, T_c, values increase with the molecular weight. However, the melting temperature, T_m, of the polymers from the second scan decreases with increasing molecular weight. Enthalpies of melting from the second scan were found to decrease in the same order.

Figure 2 represents the first DSC run for sample P3 before and after annealing at the temperatures T_a = 320 and 345 °C for 40 min. The large sharp endothermic peak remains essentially constant and a small endothermic peak appears at about 15 deg above the T_a value used, in agreement with observations for the double melting behavior.[4−6] The DSC traces for the annealed material did not show any exothermic area.

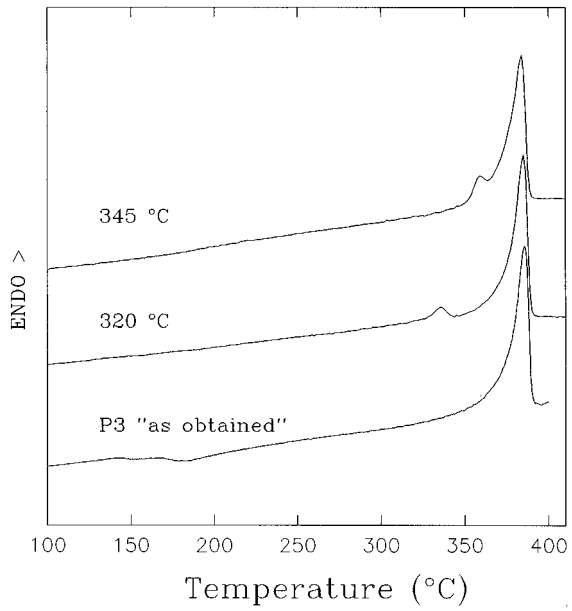

Figure 2. First DSC traces for the sample P3 before and after annealing at 320 and 345 °C for 0.7 h.

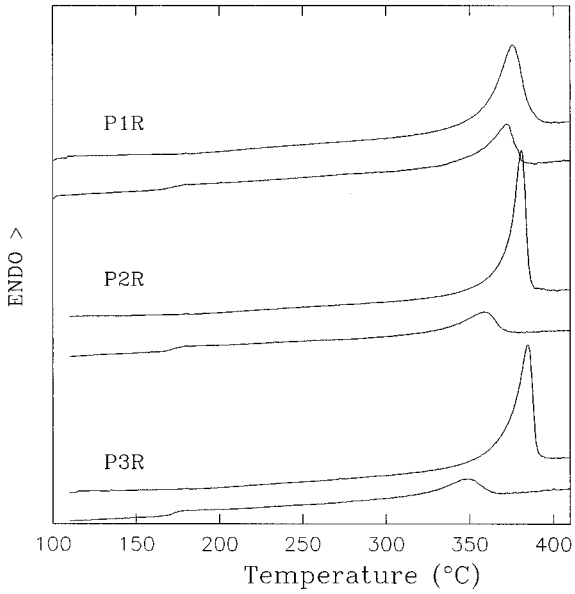

Figure 3. Same as Figure 1 but relative to the reprecipitated samples.

The as obtained polyketones consist of particles widely differing in shape and size (see Experimental Section). Therefore, reprecipitation of the polyketones from solution should erase any architectural features of the particles, thus allowing us to carry out a comparison of the physical properties of the three polymer samples under the same conditions. Figure 3 shows the first and second DSC traces of the reprecipitated samples as described in the experimental part. Their characteristic thermal properties measured are presented in Table 3. The first DSC runs show endothermic peaks similar to those of the original samples (see Figure 1 and Table 3). However, the exothermic area around 180 °C is much less pronounced than for the original samples. Concerning the second DSC runs, these do not exhibit any cold crystallization peak. The T_g and T_m values observed in the second DSC run for reprecipitated samples are systematically higher than those observed for the original samples (see Tables 2 and 3). Furthermore, a small increase of the fusion

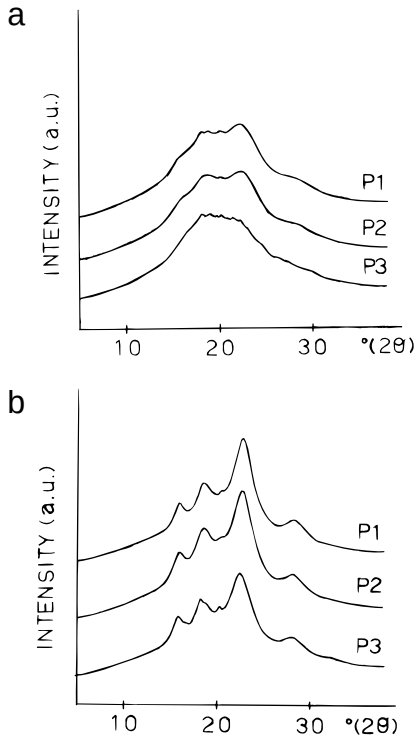

Figure 4. WAXD diffractograms for sintered polyketones samples before (a) and after (b) annealing at 230 °C for 15 min.

Table 3. Thermal Properties from the First and Second DSC Runs of "Reprecipitated" Polyketones Samples

	first DSC scan		second DSC scan		
sample	T_m (°C)	ΔH (J/g)	T_g (°C)	T_m (°C)	ΔH (J/g)
P1	375.6	64.6	168.3	372.0	32.2
P2	380.9	64.3	172.0	358.2	25.1
P3	384.7	64.5	171.6	349.0	20.3

enthalpy values was observed for the reprecipitated samples in relation to the as obtained ones.

X-ray Diffraction. Figure 4a illustrates the wide angle X-ray diffractograms from sintered samples of the three polymer particles as obtained. All three samples show poorly defined scattering patterns. P1 and P2 samples exhibit broad and weak diffraction peaks with the maximun intensity around 23° (2θ). In the case of P3 the diffractogram shows a different intensity distribution. After a thermal treatment at 230 °C for 15 min the sintered samples showed an improvement in the definition of the crystal peaks and the degree of crystallinity (Figure 4b). The diffractograms of the three samples are similar and can be considered equivalent to the scattering patterns reported for polyketones with a high carbonyl content (PEKK and PEKEKK) prepared under cold crystallization or from solvent crystallization; i.e. they exhibit the polymorphic form II. The reflection at ~15.6° (indexed as 010) appears well isolated and it allows a quick recognition of the crystallographic form II. In the case of P3 the presence of other low-intensity reflections at about 18 and 20° (2θ) points to the coexistence of both crystallographic forms (I and II).

Parts a and b of Figure 5 show the X-ray diffractograms corresponding to the sintered reprecipitated samples before and after annealing at 230 °C for 15 min. These diffractograms correspond to the polymorphic form I, which shows the strongest reflection at ~18° (indexed as 110).

Further annealing of P3 at higher temperatures provokes important changes in the relative intensity of

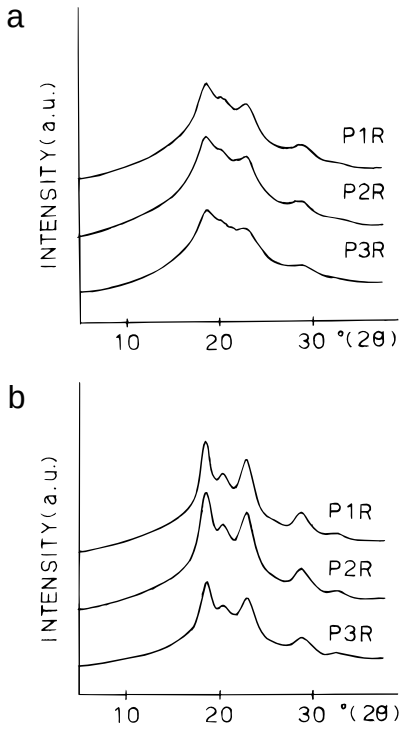

Figure 5. WAXD diffractograms for sintered, reprecipitated samples: before (a) and after (b) annealing at 230 °C for 15 min.

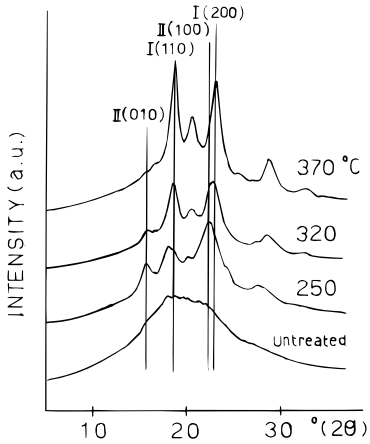

Figure 6. WAXD diffractograms for sintered sample P3 untreated and after consecutive annealing at 250, 320, and 370 °C for 15 min.

Table 4. X-ray Crystallinity in Percent of "As Obtained" and "Reprecipitated" PEKEKK Samples before and after Annealing at 230 °C for 15 min

	as obtained		reprecipitated	
sample	untreated	annealed	untreated	annealed
P1	11	26	17	25
P2	13	27	15	24
P3	9	24	13	23

the diffraction peaks (Figure 6). Thus, with increasing temperature, an intensity decrease of the peaks corresponding to form II and a concurrent intensity increase in the maxima associated with form I is observed. Form II disappears at higher temperatures (375 °C).

The X-ray crystallinity values from the as obtained and reprecipitated samples before and after annealing are presented in Table 4. The crystallinity values for the sintered samples are smaller than for the reprecipitated ones. After annealing, both the as obtained and the reprecipitated samples show similar crystallinity values. For the reprecipitated samples the degree of crystallinity appears to decrease with increasing viscosity or M_w.

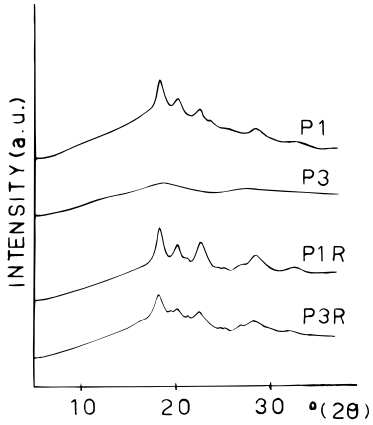

Figure 7. WAXD diffractograms for samples P1 and P3 after the second DSC run for samples before (top) and after (bottom) reprecipitation.

X-ray diffractograms were also obtained for the melt-crystallized material (samples after second DSC run). Samples as obtained showed much less defined diffractograms than the reprecipitated samples (Figure 7). Thus, while sample P1 shows a diffractogram similar to that of P1R, sample P2 shows a lower crystallinity (not included in Figure 7) and P3 can be considered amorphous.

Although sample P3 shows a large number of isolated, very small needlelike particles together with the larger ones, a separation of the needlelike particles, in a convenient amount, from the larger particles was unsuccessful. Glass capillaries with 0.7 and 2 mm diameters were filled with material from the P3 sample and the X-ray scattering patterns were obtained. While the thin capillary sample only showed a very broad ring centered around 21° (2θ), the wider one showed an X-ray pattern with well-defined rings. These results suggest that the smallest particles of P3 are mainly amorphous.

Infrared Dichroism Study. In the case of sample P3 the optical and SEM photographs reveal the presence of very small needlelike particles which show well-defined crystal habits. Nevertheless, as mentioned above, the X-ray scattering patterns of these particles reveal the occurrence of an amorphous structure. Since the appearance of crystal habits in a particle would be the result of some molecular organization during its growth, we have used infrared dichroism[16] for the investigation of these needlelike particles.

Figure 8 illustrates the polarized infrared spectra of a single needle particle of the P3 sample. The longest particle size direction was taken as the reference to apply parallel and perpendicular polarized light. We can see that those bands which can be related to the phenylene ring[17] (1589 and 1495 cm^{-1} (ν_{C-C}), 1162 and 927 cm^{-1} (out of plane H vibration mode in the paraphenylene ring)) and the set of bands (1309, 1276 and 1235 cm^{-1}) associated with the phenylene linked to the keto group[18] and aromatic ether group show a remarkable dichroism. The intensity of these bands is much larger for parallel polarized light. On the contrary, the band at 1657 cm^{-1}, associated with the keto group[17] shows a very small dichroism and the band intensity is slightly larger for the perpendicular polarization.

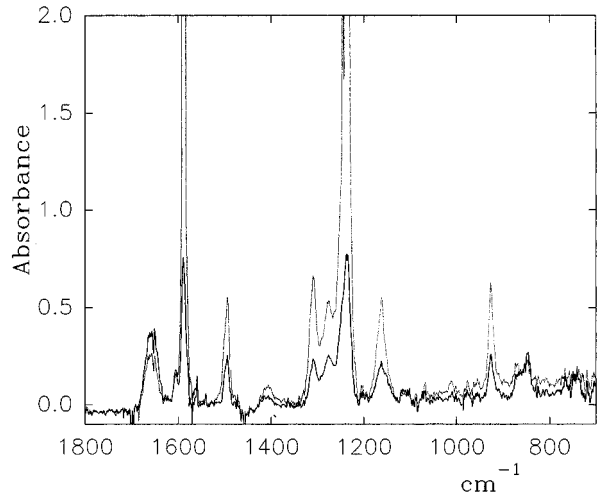

Figure 8. Polarized infrared spectra of a single needlelike particle of P3 sample: (dotted line) ∥; (solid line) ⊥.

Discussion

The above results will be discussed with reference to the influence of polymerization conditions on the thermal properties and to the microstructure of the particles as obtained and of their modification after annealing and reprecipitation. The influence of molecular weight (viscosity) and isomeric defect structures on the architecture of particles as obtained and their thermal properties will also be pointed out.

(a) Thermal Properties. The DSC thermograms of the obtained polyketones reveal the melting behavior which is typical of semicrystalline polymers. It is to be noted that the thermal properties measured from both the first and second heating DSC scans seem to depend mainly on molecular weight (Table 2). Hence, an increase of molecular weight (viscosity) results in an increase of the melting points observed in the first DSC scan. Furthermore, a broader endothermic peak is observed for sample P1 which shows the smallest viscosity value but the highest amount of defect structures (Table 1). Thus, a contribution of defect structures to the observed lowering of T_m (from P1 to P3) cannot be discarded. According to the second DSC runs the T_g values increase with molecular weight as expected. However, the T_m values decrease with increasing molecular weight. This could indicate a decreasing size or quality of the crystals grown on cooling the sample after melting. Such an effect could be due to a decreasing chain mobility going from P1 to P3 because of the differences observed in molecular weight.

It is worthwhile to compare the thermal behavior observed for samples as obtained (Figure 1 and Table 2) with that of the reprecipitated samples (Figure 3 and Table 3). As illustrated elsewhere,[15] the samples show very different morphologies when observed by optical microscopy.

By reprecipitation of the samples we are erasing the likely influence of the particles architecture on the thermal properties which will reflect, in turn, the influence of molecular weight and microstructure of the sample. Since weight losses during reprecipitations are small (less than 2.5%), the chemical composition of the reprecipitated polyketones should be assumed to be identical to that of the obtained polyketones. On the whole, a systematic increase of T_m and T_g and enthalpic values was found for the reprecipitated samples in relation to the as obtained ones. Besides the changes observed in T_m and Tg values after reprecipitation of the samples (see Tables 2 and 3) the corresponding second DSC runs reveal a clear different thermal behavior between as obtained and reprecipitated samples. In the first case, a cold crystallization peak is observed for the three samples, while in the case of reprecipitated samples, the cold crystallization peak is not observed. This result could be attributed to a different ability of the samples to crystallize on cooling after the first DSC run. Hence, the capability for crystallization is total in the case of reprecipitated samples and only partial for as obtained samples. Thus, the cold crystallization enthalpy values are smaller than the melting enthalpies for P1 and P2 samples (Table 2) while for P3 these values are similar. The difference between both crystallization and melting enthalpies is much larger for P1 (22 J/g) than for P2 (6.6 J/g) and nil for P3.

Table 5. Influence of Sample Preparation on the Polymorphism in PEKEKK Materials

			melt crystallized	
	as obtained	reprecipitated	as obtained	reprecipitated
P1	form II + (form I)[a]	form I	form I	form I
P2	form II + (form I)[a]	form I	form I[c]	form I
P3	form II + form I[b]	form I	amorphous	form I

[a] Form I could not be ruled out. [b] Form II is dominant. [c] Sample with very low crystallinity.

(b) Polymorphism and Crystallization Conditions. The variations observed in the X-ray diffractograms (Figure 6) and diffraction patterns upon annealing of the samples are in line with the polymorphism observed in related polyketones. We can say that the as obtained samples appear predominantly in the crystallographic form II, though the presence of form I is not ruled out. Upon annealing, a crystal transformation of form II into form I occurs. This crystal conversion seems to be more effective for higher annealing temperatures and also for longer thermal treatments, as expected. It is worth noting that polyketones as obtained, i.e. crystallized from solution reaction (precipitation polycondensation), exhibit mainly form II (see Figure 4) while the reprecipitated samples show only form I (Figure 5).

The X-ray diffractograms obtained from the melt-crystallized samples (from DSC measurements after the second run) clearly support the above mentioned differences between reprecipitated and as obtained samples (Figure 7). In the case of samples as obtained only sample P1 shows X-ray scattering patterns similar to those of reprecipitated samples while the diffractogram of sample P2 (not shown in the figure) denotes a very low crystallinity level and that of sample P3 would correspond to an amorphous material. In the case of reprecipitated samples the X-ray diffractograms reveal a similar semicrystalline character for all three samples. It is noteworthy that the X-ray diffractograms of melt-crystallized material correspond to form I, in agreement with Gardner's observations. Table 5 summarizes the influence of the preparation conditions on the polymorphism observed in these polyketone materials containing a proportion of carbonyl linkage groups of 60%.

(c) Arrangement of the Polyketone Chains in the Needlelike Particles. It is worthwhile to recall the amorphous character exhibited by the smallest particles of sample P3 (which showed birefrigence and crystal habit), while larger P3 particles are semicrystalline. A short thermal treatement of the sample is sufficient to develop crystallinity in these particles. This indicates that for this particular sample having a very

much higher viscosity (molecular weight) the still growing chains in the precipitated particles could not pack properly (i.e. in crystallographic register), yielding both amorphous and poorly semicrystalline material. However, results obtained from IR dichroism indicate that polymer chains are aligned parallel to the longest dimension of the needle particle. Taking into account the chain conformation of linear polyketones in which ether and keto groups, linking para-phenylene rings, are on the edges of an all-trans planar conformation,[7−10] the infrared results shown in Figure 8 can be explained if polyketone chains lie parallel along the longest particle dimension. Furthermore, the chains would laterally pack at random which would result in a uniaxial orientation with the main axis parallel to the direction of the longest particle size. As a result the C−C and C−H bonds of the phenylene rings would show a permanent dipolar moment parallel to the chain direction and, consequently, their associated IR bands will exhibit dichroism. On the other hand, since the stretching vibration mode of the C=O bond is perpendicular to the chain direction and because of uniaxial orientation of needle particles, the corresponding band at 1657 cm^{-1} will not exhibit such a high dichroism. Indeed, only a small dichroism is observed for the ν_{CO} band at 1657 cm^{-1}.

(d) Isomeric Chain Defects and Chain Entanglements. From the foregoing the influence of molecular weight on the chain mobility is evident. Chain mobility is, in turn, responsible for the thermal behavior observed and it determines the ability of chains to crystallize from the melt. However, even if the relative amount of defect structures is small (Table 1), their influence on the architecture developed in the growing precipitated particles cannot be discarded. One may speculate that the presence of defect structures (ortho and meta) might be responsible for an entanglement between growing chain segments. Chain entanglements could be released by reprecipitation of the samples, allowing the material to crystallize better, as indicated by the higher enthalpy and T_m values observed in relation to those for as obtained samples.

Taking into account the relatively high viscosity values observed for the three samples (Table 1) and given the low flexibility of polyketone chains one could attribute the increasing T_m values not exclusively to the changes in M_w (viscosity) but also to the smaller amount of defect structures found when going from P1 to P3.

One might think that reprecipitated polymers could crystallize from the melt more easily than as obtained ones do, as occurs here. One may speculate that this could be due to a chain disentanglement during polymer solution which would increase the chain mobility in the reprecipitated polymers in relation to that of as obtained polyketones.

Conclusions

The level of crystallinity and the melting behavior of the polyketones investigated primarily depends on the molecular weight. Similar to other polyketones, PEKEKK shows two polymorphic forms: form II, less stable, is currently observed in the samples, while the reprecipitated polymer preferentially shows form I. Form II is partially converted into form I upon short annealing treatment of the material, and it is totally converted after crystallization from the melt. The crystallinity of samples seems to decrease with increasing molecular weight (viscosity), while the corresponding melting temperatures increases. Second DSC runs show decreasing T_m values with increasing molecular weight in both as obtained and reprecipitated samples. This result highlights the influence of molecular weight on the chain mobility and consequently on the crystallization process from the melt as well as the thermal behavior observed upon heating. Similarly to molecular weight, isomeric defects in the chains also seem to govern the building up of the particles, thus affecting the chain mobility which finally determines the thermal behavior and the ability of chains to crystallize.

Acknowledgment. Grateful acknowledgment is due to DGICYT, Spain, for the support of this investigation (grant PB94-0049). M.G.Z. also thanks DGICYT for the tenure of a sabbatical grant during his research work in Madrid.

References and Notes

(1) Staniland, P. A. In *Comprehensive Polymer Science*; Allen, G., Bevington, J. C., Eds.; Pergamon: Oxford, U.K., 1989; Vol. 5, pp 483−497.
(2) Millins, M. J.; Woo, E. P. *J. Macromol. Sci.-Rev. Macromol. Chem. Phys.* **1987**, *C27*, 313.
(3) *Handbook of polymer synthesis, Part A*; Kricheldorf, H. R., Eds.; Marcel Dekker: New York, 1992; p 545.
(4) Blundell, D. J.; Osborn, R. N. *Polymer* **1983**, *24*, 953.
(5) Cheng, S. Z. D.; Cao, M. Y.; Wunderlich, B. *Macromolecules* **1986**, *19*, 1868.
(6) Bassett, D. C.; Olley, R. H.; Al Raheil, I. A. M. *Polymer* **1988**, *29*, 1745.
(7) Boom, J.; Magre, E. P. *Makromol. Chem.* **1969**, *126*, 130.
(8) Dawson, P. C.; Blundell, D. J. *Polymer* **1980**, *21*, 577.
(9) Rueda, D. R.; Ania, F.; Richarson, A.; Ward, I. M.; Baltá-Calleja, F. J. *Polym. Commun.* **1983**, *24*, 258.
(10) Wakelyn, N. T. *Polym. Commun.* **1984**, *25*, 306.
(11) Blundell, D. J.; Newton, A. B. *Polymer* **1991**, *32*, 308.
(12) Gardner, K. H.; Hsiao, B. S.; Matheson, R. R., Jr.; Wood, B. A. *Polymer* **1992**, *33*, 2483.
(13) Gardner, K. H.; Hsiao, B. S.; Faron, K. L. *Polymer* **1994**, *35*, 2290.
(14) Cheng, S. Z. D.; Ho, R. M.; Hsiao, B. H.; Gardner, K. H. *Macromol. Chem. Phys.* **1996**, *197*, 185.
(15) Zolotukhin, Z.; Rueda, D. R.; Bruix, M.; Cagiao, M. E.; Baltá-Calleja, F. J.; Bulai, A.; Gileva, N. G. Submitted for publication to *Macromol. Chem. Phys.*
(16) Zbinden, R. *Infrared Spectroscopy of High Polymers*; Academic Press: New York, London, 1964.
(17) Bellamy, L. J. *The infrared Spectra of Complex Molecules*, 3rd ed.; Chapman and Hall: London, 1979.
(18) Colthup, N. B. *J. Opt. Soc. Am.* **1952**, *40* (6), 397.

MA960482S